



Supplement of

Nitro-polycyclic aromatic hydrocarbons – gas–particle partitioning, mass size distribution, and formation along transport in marine and continental background air

Gerhard Lammel et al.

Correspondence to: Gerhard Lammel (lammel@recetox.muni.cz)

The copyright of individual parts of the supplement might differ from the CC-BY 3.0 licence.

Supplementary Material

Nitro-polycyclic aromatic hydrocarbons - gas-particle partitioning, mass size distribution, and formation along transport in marine and continental background air in Europe

Gerhard Lammel ^{1,2*}, Marie D. Mulder ¹, Pourya Shahpoury ², Petr Kukučka ¹, Hanka Lišková ¹, Petra Příbylová ¹, Roman Prokeš ¹, Gerhard Wotawa ³

¹ Research Centre for Toxic Compounds in the Environment, Masaryk University, Brno, Czech Republic

² Max Planck Institute for Chemistry, Mainz, Germany

³ Zentralanstalt fuer Meteorologie und Geodynamik, Wien, Austria

S1 Methodology - Organic trace analytical quality assurance parameters

The instrument limit of quantification (ILOQ), which is based on 3 times the instrument limit of detection, which in turn is based on 3 times the chromatogramme baseline noise level, was 0.002-0.033 ng for NPAHs (except for 1NNAP for which it was 0.414 ng) and 0.006-0.06 ng for 4-ring PAHs (except for FLT and PYR for which it was 0.282 and 0.115 ng, respectively) (Table S1).

Table S1: Recoveries including their relative standard deviations (RSD) (a), instrument limits of quantification (LOQ) (b), given as masses and concentrations, the latter for a typical sample volume (650 m³; range of sample volumes: 612-3130 m³ at the marine site and 578-885 m³ at the continental site) and (c) field blank values for various type of sampling media (pg)

a.

Analyte	Recovery (%)	RSD (%)
D8-NAP	72	14
D10-PHE	95	12
D12-perylene	102	9
1NNAP	70	14
2NNAP	71	16
3NACE	85	12
5NACE	83	9
2NFLU	89	14
9NPHE	91	20
3NPHE	90	16
9NANT	88	15
2NFLT	92	9
3NFLT	88	13
1NPYR	110	12
2NPYR	105	16
7NBAA	99	19
6NCHR	89	9

b.

Analyte	mass (ng)	concentration ($\mu\text{g m}^{-3}$)
FLT	0.282	0.43
PYR	0.115	0.18
BBN	0.006	0.010
BAA	0.014	0.021
TPH	0.031	0.048
CHR	0.060	0.092
1NNAP	0.414	0.64
2NNAP	0.014	0.021
3NACE	0.002	0.004
5NACE	0.005	0.008
2NFLU	0.005	0.008
9NPHE	0.033	0.051
3NPHE	0.005	0.008
9NANT	0.005	0.008
2NFLT ^a	0.025	0.038
1NPYR	0.007	0.011
2NPYR	0.005	0.008
7NBAA	0.005	0.008
6NCHR	0.005	0.008

c.

Analyte	PUF (n = 4 ^b)	QFF	
		0.49-10 μm stages (n = 4 ^b)	backup filter (n = 4 ^b)
FLT	1046±220	496±98	509±116
PYR	602±148	172±64	153±33
BBN	57±19	20±9	16±3
BAA	66±13	20±14	14±5
TPH	89±26	42±10	40±9
CHR	147±41	90±42	73±12
1NNAP	<410	72±124	363±17
2NNAP	50±44	54±12	60±1
3NACE	< 5.0	< 5.0	< 5.0
5NACE	< 5.0	< 5.0	< 5.0
2NFLU	< 5.0	< 5.0	< 5.0
9NPHE	< 5.0	< 5.0	< 5.0
3NPHE	< 5.0	< 5.0	< 5.0
9NANT	22±19	60±68	81±78
2NFLT ^a	45±39	53±8	68±1
1NPYR	14±12	15±93	21±1
2NPYR	< 5.0	< 5.0	5.5±0.7
7NBAA	< 5.0	< 5.0	< 5.0
6NCHR	< 5.0	< 5.0	< 5.0

^a co-eluted with 3NFLT, assuming $c_{3NFLT} = 0$

^b 3 PUF, 10 QFF for the stages corresponding to 0.49-10 μm and 2 QFF for particles <0.49 μm at the continental site

S2 Results

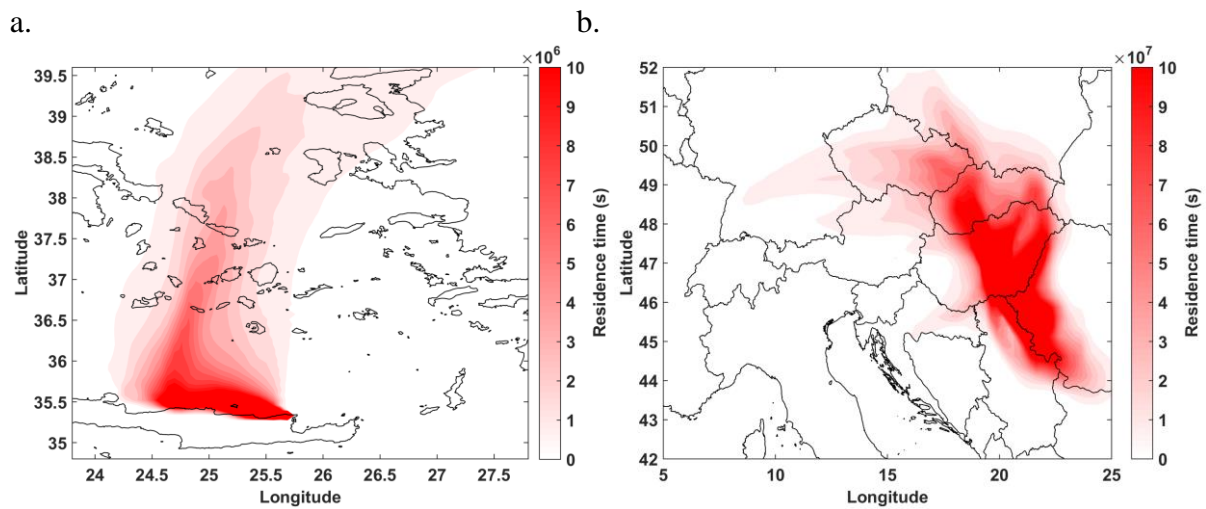
S2.1 Meteorology and transports

S2.1.1 Meteorological situations

Marine site: During 2-11 July 2012 the Aegean was mostly influenced by northerly, and in its northern part easterly advection over the Marmara Sea as part of a cyclonic system which resided over Romania during 1-3 July and moved over western Russia during 4-10 July. The sky was cloud-free all the time. No frontal passage occurred, such that for all samples taken in the study region the hypothesis of horizontal homogeneity of air mass collected can be applied. Under the influence of a strong westerly flow towards Europe the flow in the northern part of the Aegean switched to westerly during the night 11-12 July, such that air which was residing over the SW Balkans was advected as well as air from beyond, i.e. central Italy and the NW Mediterranean Sea and the Iberian Peninsula.

Continental site: During 5-16 August 2013 mostly northwesterly and northerly flow, directed by anti-cyclonic systems slowly moving eastward over northern France, Germany and Poland dominated the flow to the Gt. Hungarian Plain. These air masses travelled over industrialised areas of Hungary (Budapest), Slovakia, Czech Republic, Germany and Poland. During 10-13 August advection from southeast contributed, too.

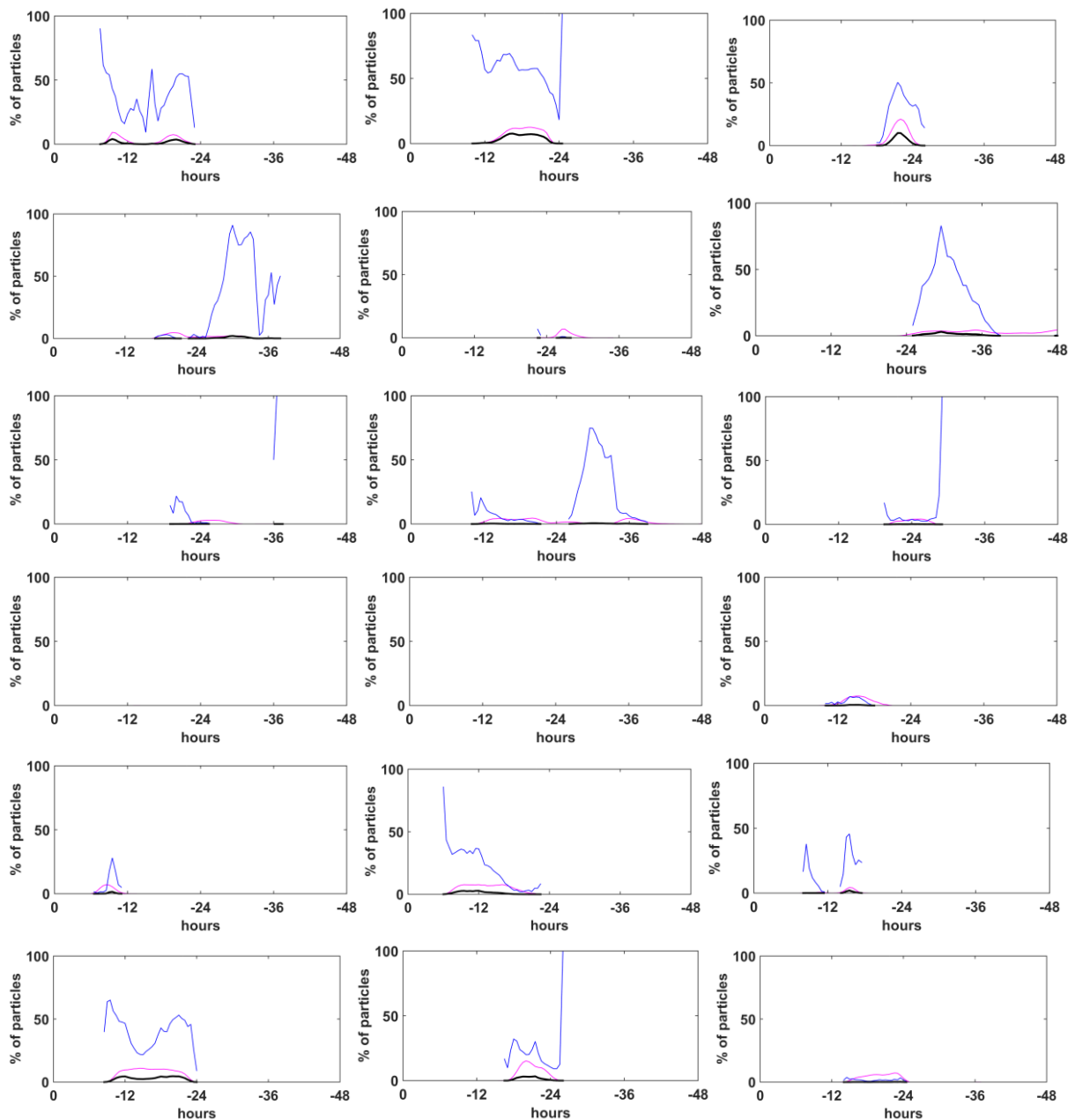
Fig. S1. Back trajectories from the (a) marine and (b) continental site during the measurements in summers 2012 and 2013, respectively. FLEXPART simulations 48 h backward in time.



S2.1.2 Quantification of urban influence on samples

As an implication of the impactor sampling protocol at the marine site, individual samples encompass up to 4 days/nights. The sampling periods selected for the sub-dataset representing marine background conditions are the day-times 7 and 13 July and the nights of 6-7 and 11-12 July (i.e. samples No. 9, 10, 19 and 22 in Fig. S3), while the sampling periods selected for the sub-dataset representing background with urban influence are the day-times 3 and 10 July and the nights 2-3 and 10-11 July (i.e. samples No. 1, 2, 16 and 17 in Fig. S3).

Fig. S2. Tracking of urban influence in air mass history: Fraction of Lagrangian particles (or air parcels) continuously released in FLEXPART runs, travelling from the marine site back in time that crossed the Izmir area (purple), the fraction of these particles which had crossed the Izmir area within the boundary layer (blue), and product of these two fractions (black) for arrival time periods. 22 sequential day/night samples 2-13 July 2012.



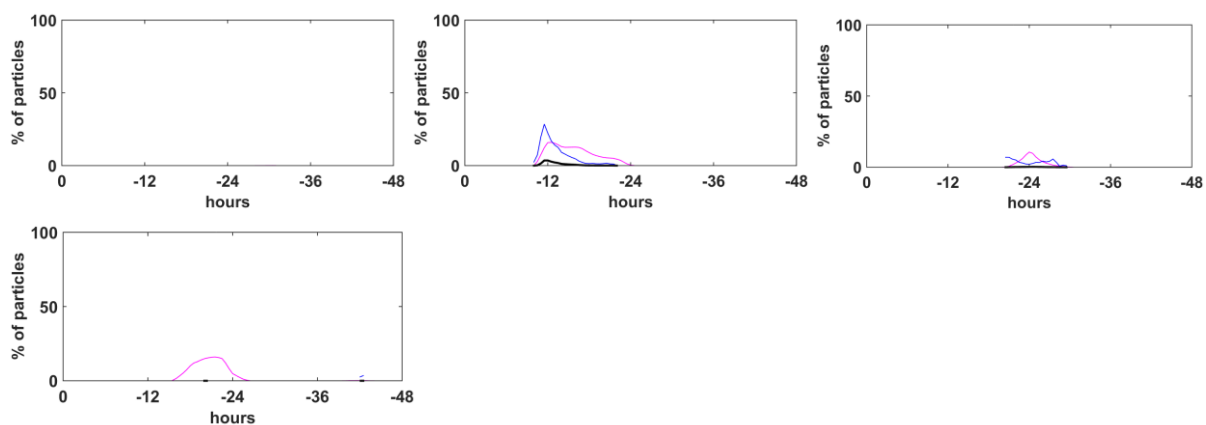
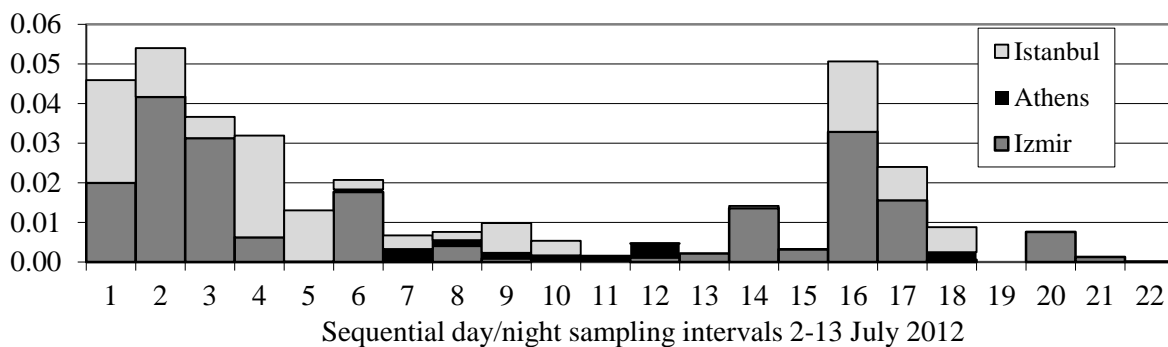
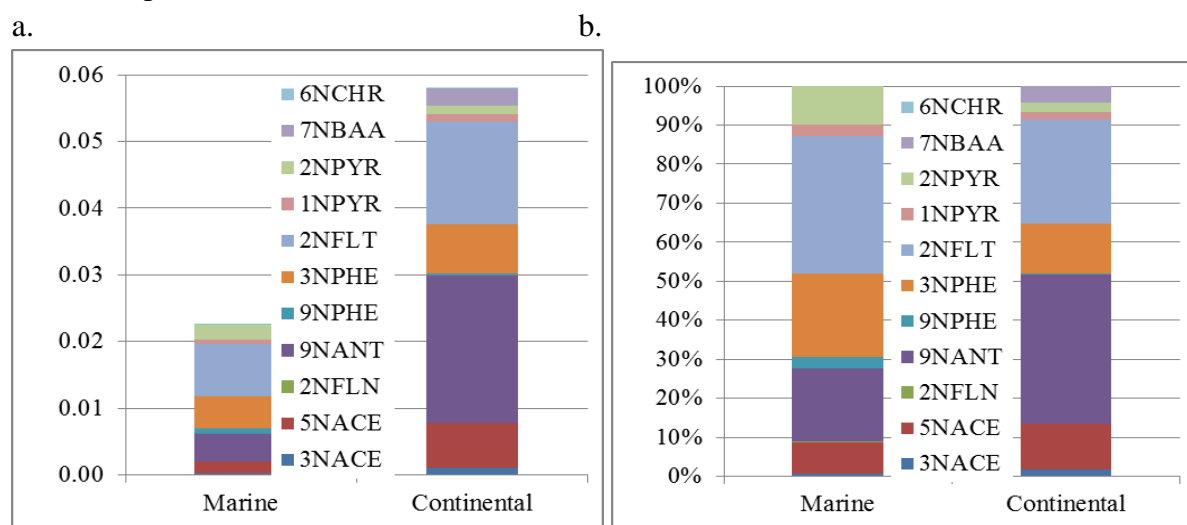


Fig. S3. Tracking of urban influence in air mass history: Time series of urban dose, D_u , of samples collected at the marine site on the Island of Crete related to transport passing Izmir (≈ 300 km direct distance, $38.2-38.8^\circ\text{N}/26.2-27.3^\circ\text{E}$), Athens (≈ 300 km, $37.8-38.1^\circ\text{N}/23.5-23.8^\circ\text{E}$) and Istanbul (≈ 500 km away, $40.8-41.1^\circ\text{N}/28.6-29.5^\circ\text{E}$). FLEXPART simulations 48 h backward in time (see Fig. S2).



S2.2 Concentrations

Fig. S4: Mean absolute (a; ng m^{-3}) and relative (b) total (gas + particulate) 2-4 ring NPAH substance patterns at the marine and continental sites



S2.3 Gas-particle partitioning

S2.3.1 Prediction by ppLFER

Deviations between predicted and observed (Fig. 3):

Root-mean square errors (RMSE) of $\log K_p$ ($\text{m}^3 \text{g}^{-1}$) predictions by the poly-parameter linear free energy relationship (ppLFER) model for 5NACE, 1NPYR, 2NPYR, and 2NFLT were 1.63, 1.48, 1.49, and 0.81, respectively, at the marine site. At the continental site, the RMSE values for 5NACE, 9NANT, 9NPHE, 3NPHE, 2NPYR, 3NACE, and 2NFLT were between 0.50 and 0.84, and 1.11 and 1.86 for 1NPYR and 7NBAA, respectively.

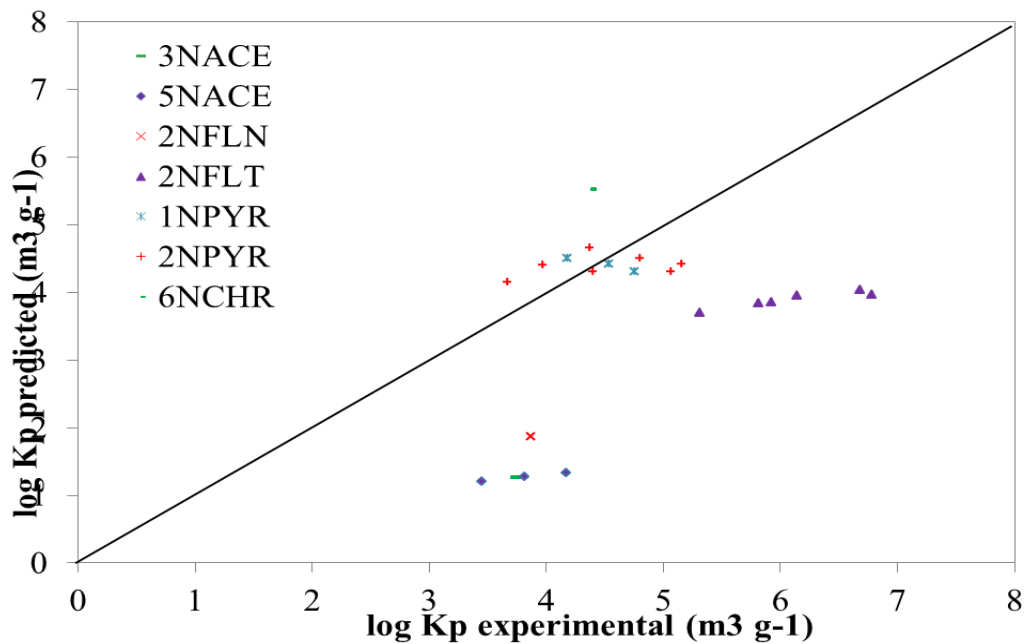
S2.3.2 Prediction by spLFER

A single-parameter linear free energy relationship (spLFER), namely the K_{oa} model (Finizio et al., 1997) was applied. This model was slightly modified, as K_{oa} and enthalpies of liquid-gas phase transfer were derived using Abraham solute descriptors and ppLFER equations suggested by Abraham et al. (2010) and Mintz et al. (2007). The model is presented in detail and discussed in Shahpoury et al., 2016, and Tomaz et al., 2016.

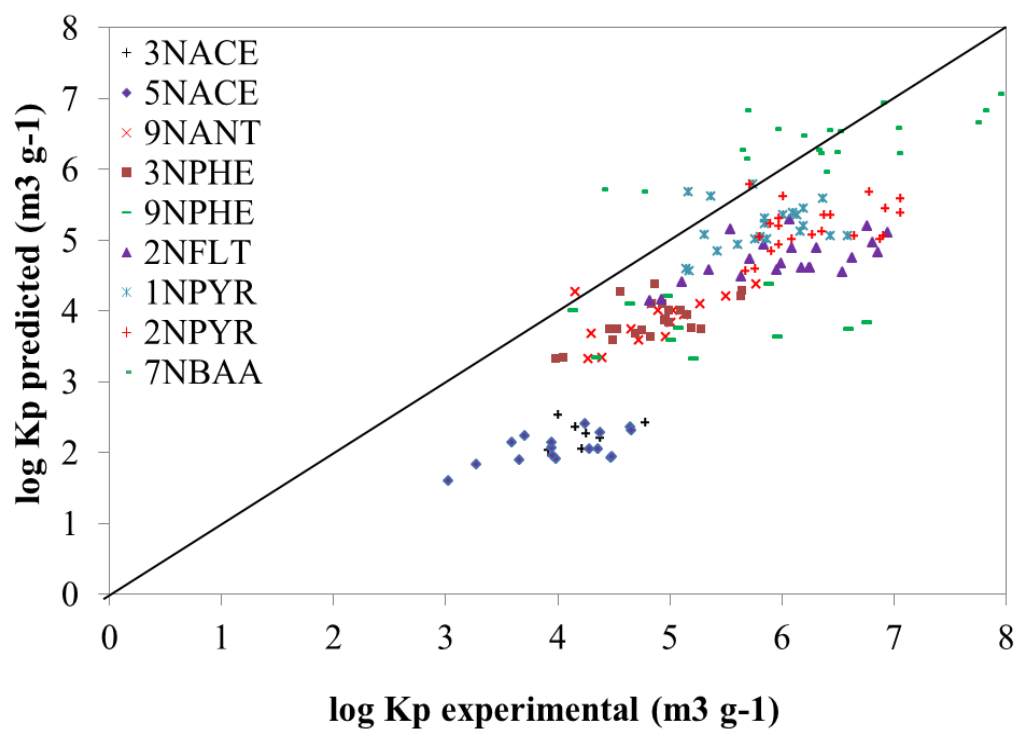
Deviations between predicted and observed (Fig. S5): At the marine site, the RMSE values of $\log K_p$ ($\text{m}^3 \text{g}^{-1}$) predictions by the spLFER were 0.9 and 1.3 log-units larger than determined for ppLFER predictions (S2.3.1, above) for 5NACE and 2NFLT, respectively, and were 1.1 and 1.0 log-units smaller for 1NPYR and 2NPYR, respectively. At the continental site, the RMSE values were between 0.2 and 0.9 log-units larger than the values determined for ppLFER predictions (S2.3.1, above), with the exception of 1NPYR and 7NBAA for which the RMSE values were 0.4 and 1.1 log-units smaller.

Fig. S5. Predicted versus experimental $\log K_p$ ($\text{m}^3 \text{air g}^{-1} \text{PM}$) for NPAHs using the K_{oa} model at the (a) marine and (b) continental sites

a.



b.



References

- Abraham, M.H., Smith, R.E., Luchtefeld, R., Boorem, A.J., Lou, R., Acree, W.E., 2010. Prediction of solubility of drugs and other compounds in organic solvents. *J. Pharm. Sci.* 99, 1500–1515.
- Finizio, A., Mackay, D., Bidleman, T., Harner, T., 1997. Octanol-air partition coefficient as a predictor of partitioning of semi-volatile organic chemicals to aerosols. *Atmos. Environ.* 31, 2289–2296.
- Mintz, C., Clark, M., Acree, W.E., Abraham, M.H., 2007. Enthalpy of solvation correlations for gaseous solutes dissolved in water and in 1-octanol based on the Abraham model. *J. Chem. Inf. Model.* 47, 115–121.
- Shahpoury, P., Lammel, G., Albinet, A., Sofuoğlu, A., Dumanoğlu, Y., Sofuoğlu, S.C., 2016. Model evaluation for gas-particle partitioning of polycyclic aromatic hydrocarbons in urban and non-urban sites in Europe – Comparison between single- and poly-parameter linear free energy relationships based on a multi-phase aerosol scenario. *Environ. Sci. Technol.* 50, 12312-12319.
- Tomaz, S., Shahpoury, P., Jaffrezo, J.L., Lammel, G., Perraudin, E., Villenave, E., Albinet, A. (2016) One year study of polycyclic aromatic compounds at an urban site in Grenoble (France): seasonal variations, gas/particle partitioning and cancer risk estimation, *Sci. Total Environ.* 565, 1071-1083.